

弹性支撑浅拱的非线性动力行为分析*

易壮鹏^{1†} 康厚军² 王连华²

(1. 长沙理工大学土木与建筑学院, 长沙 410114) (2. 湖南大学土木工程学院, 长沙 410082)

摘要 本文研究了两端转角均为转动弹簧支撑的铰支浅拱在外激励作用下的非线性动力学行为. 基于弹性支撑浅拱的基本动力控制方程, 采用多尺度法对内共振进行了摄动分析, 并得到了极坐标形式的平均方程. 弹性约束的刚度通过特征方程影响结构的自振频率和模态, 且与平均方程的相关系数一一对应, 文中还以最低两阶模态之间 1:1 内共振为对象进行了数值分析. 结果显示系统存在模态交叉与转向两种内共振形式, 另一方面结构参数处于某一范围之内时外激励激发的模态作用可导致出现准周期运动和混沌运动.

关键词 浅拱, 转动弹性支撑, 内共振, 分岔, 模态转向

DOI: 10.6052/1672-6553-2013-020

引言

拱结构^[1]线形优美、受力性能良好, 有着广泛的工程背景. 国内外学者对各种外荷载作用下的静、动力学进行了深入的研究, 涉及到几何缺陷^[2]、承载能力^[3-5]、跳跃屈曲^[6-7]及分岔混沌^[8-10]等各个方面. 这些研究中, 拱的边界一般假定为理想的固支或铰支, 实际上在工程实践中拱的边界在某些情况下不能简单地视为铰支或固支, 如柔性系杆拱中存在系杆使得其力学模型可抽象为水平弹性支撑拱; 另外一些机械拱臂或曲臂是存在平动和转动的弹性约束. 对于弹性和粘弹性边界结构的研究主要集中于梁^[11-12], 较少涉及到拱的动力行为. 由于拱结构与相邻结构共同承受载荷, 动力荷载下基础变形引起附加惯性力, 将对结构的动力响应产生影响, 因此采用弹性支撑边界来研究结构的动力行为更加合理. 本文以两端转动弹性约束浅拱为研究对象, 采用多尺度法^[13]分析最低两阶模态之间的 1:1 内共振现象及相应的分岔、混沌等非线性动力学行为.

1 分析模型

1.1 基本方程

图 1 所示直角坐标系 $\delta - \hat{x}\hat{y}$ 下跨径为的两端转动弹性支撑浅拱, 弹簧刚度分别为 \hat{k}_1 和 \hat{k}_2 , \hat{y}_0

(\hat{x}) 为初始时刻的拱轴线, $\hat{y}(\hat{x}, t)$ 为 t 时刻在外荷载 $f(\hat{x}, t)$ 作用下的位置. 引入基本假定(1)平截面假定; (2)不考虑剪切变形和转动惯量; (3)零初始轴向力, 动力学控制方程可写为^[13]:

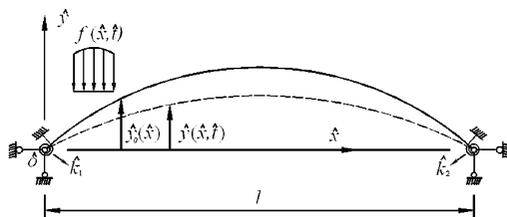


图 1 转动弹性支撑浅拱结构示意图

Fig. 1 The schematic torsional spring support shallow arch and the excitation

$$\rho A \frac{\partial^2 \hat{y}}{\partial t^2} + EI \frac{\partial^4 \hat{y}}{\partial \hat{x}^4} - \frac{EA}{l} \frac{d^2 \hat{y}_0}{d\hat{x}^2} \int_0^l \frac{\partial \hat{y}}{\partial \hat{x}} \frac{d\hat{y}}{d\hat{x}} d\hat{x} = \frac{EA}{l} \frac{\partial^2 \hat{y}}{\partial \hat{x}^2} \int_0^l \frac{\partial \hat{y}}{\partial \hat{x}} \frac{d\hat{y}_0}{d\hat{x}} d\hat{x} + \frac{EA}{2l} \frac{d^2 \hat{y}_0}{d\hat{x}^2} \int_0^l \left(\frac{\partial \hat{y}}{\partial \hat{x}} \right)^2 d\hat{x} + \frac{EA}{2l} \frac{\partial^2 \hat{y}}{\partial \hat{x}^2} \int_0^l \left(\frac{\partial \hat{y}}{\partial \hat{x}} \right)^2 d\hat{x} - \hat{c} \frac{\partial^2 \hat{y}}{\partial t} - f(\hat{x}, t) \quad (1)$$

其中 A 为截面积, I 为转动惯量, ρ 为密度, E 为弹性模量, \hat{c} 为阻尼系数, 边界条件为:

$$\hat{x}=0: \quad \hat{y}=0, EI \frac{\partial^2 \hat{y}}{\partial \hat{x}^2} - \hat{k}_1 \frac{\partial \hat{y}}{\partial \hat{x}} = 0 \quad (2)$$

$$\hat{x}=l: \quad \hat{y}=0, EI \frac{\partial^2 \hat{y}}{\partial \hat{x}^2} + \hat{k}_2 \frac{\partial \hat{y}}{\partial \hat{x}} = 0 \quad (3)$$

2012-10-12 收到第 1 稿, 2012-11-27 收到修改稿.

* 国家自然科学基金资助项目 (11002030, 10972073, 11102063, 11032004); 教育部新世纪人才项目 (NCET-09-0335)

† 通讯作者 E-mail: yizhuangpeng@163.com

引入如下无量纲参变量

$$x = \frac{\hat{x}}{l}; \quad \psi = \frac{\hat{y}_0}{r}; \quad u = \frac{\hat{y}}{r}; \quad t = \hat{t} \sqrt{\frac{EI}{\rho A l^4}} \quad (4)$$

其中 r 是截面的转动惯量, 方程可无量纲化如下

$$\begin{aligned} \frac{\partial^2 u}{\partial t^2} + \frac{\partial^4 u}{\partial x^4} - \frac{d^2 \psi}{dx^2} \int_0^1 \frac{\partial u}{\partial x} \frac{d\psi}{dx} dx &= \frac{\partial^2 u}{\partial t^2} \int_0^1 \frac{\partial u}{\partial x} \frac{d\psi}{dx} dx + \\ \frac{1}{2} \frac{d^2 \psi}{dx^2} \int_0^1 \left(\frac{\partial u}{\partial x} \right)^2 dx &+ \frac{1}{2} \frac{\partial^2 u}{\partial t^2} \int_0^1 \left(\frac{\partial u}{\partial x} \right)^2 dx - \\ \varepsilon^2 c \frac{\partial u}{\partial t} - \varepsilon^3 F \cos \Omega t & \end{aligned} \quad (5)$$

式中 ε 是无量纲小参数, $\varepsilon^2 c = l^2 / \sqrt{\rho A E I} \hat{c}$, $\varepsilon^3 F \cos \Omega t = (l^4 / E I r) f(\hat{x}, \hat{t})$ 为谐波激励, $\varepsilon^3 F$ 是其幅值, 方程对应的边界为

$$u = 0, \quad \frac{\partial^2 u}{\partial x^2} - k_1 \frac{\partial u}{\partial x} = 0 \quad \text{at} \quad x = 0 \quad (6)$$

$$u = 0, \quad \frac{\partial^2 u}{\partial x^2} + k_1 \frac{\partial u}{\partial x} = 0 \quad \text{at} \quad x = 1 \quad (7)$$

其中 $k_1 = \hat{k}_1 l / EI$ 和 $k_2 = \hat{k}_2 l / EI$ 是无量纲转动弹簧刚度, 并在后续摄动分析中假定为 $O(1)$.

1.2 自振特性

将式(5)中阻尼、外荷载和非线性项去掉, 可得用于分析结构自振频率和模态的方程

$$\frac{\partial^2 u}{\partial t^2} + Lu = \frac{\partial^2 u}{\partial t^2} + \frac{\partial^4 u}{\partial x^4} - \frac{d^2 \psi}{dx^2} \int_0^1 \frac{\partial u}{\partial x} \frac{d\psi}{dx} dx = 0 \quad (8)$$

边界条件仍为(6)和(7), 上式中是为了计算方便引入的正线性自伴微分算子. n 阶频率 ω_n 对应正交模态 $\phi_n(x)$, 将其标准化有 $\int_0^1 \phi_m \phi_n dx = \langle \phi_m, \phi_n \rangle = \delta_{mn}$ (δ 函数), $\langle \phi_m, L\phi_n \rangle = \omega_n^2 \delta_{mn}$. 无量纲浅拱方程可假定为 $\psi(x) = b \sin \psi x$, b 为矢高, 正交模态可以表示为

$$\begin{aligned} \phi_n(x) &= c_1 \cos \omega_n^{1/2} x + c_2 \sin \omega_n^{1/2} x + c_3 \cosh \omega_n^{1/2} x + \\ &c_4 \sinh \omega_n^{1/2} x + c_5 \sin \pi x \end{aligned} \quad (9)$$

其中 c_i 满足(6-8)式的特征方程的系数, ω_n 是特征解, 详细表达式见附录(A1-A5)式.

为考察结构参数变化时自振频率的分布规律, 图2给出了转动约束弹簧刚度 k_1 和 k_2 取两组不同值时各阶频率随矢高 b 的变化图. 从中可看到, 相邻阶次模态之间可能发生模态交叉(cross)或转向(veer)的1:1内共振, 且(a) $k_1 = 10, k_2 = 10$ 时两种形式在各递增的相邻模态间交替出现, (b) $k_1 = 10,$

$k_2 = 20$ 时各相邻模态间只有模态转向, 这与两端铰支或固支^[14]的模态形式存在明显差异.

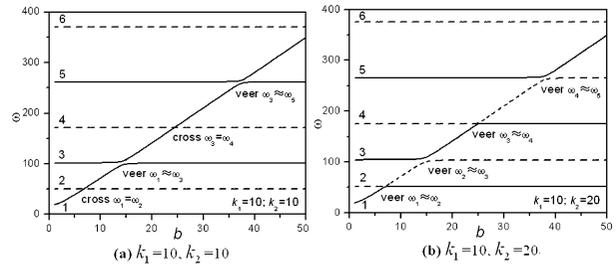


图2 频率随矢高的变化示意图

Fig. 2 Variation of frequencies with arch rise

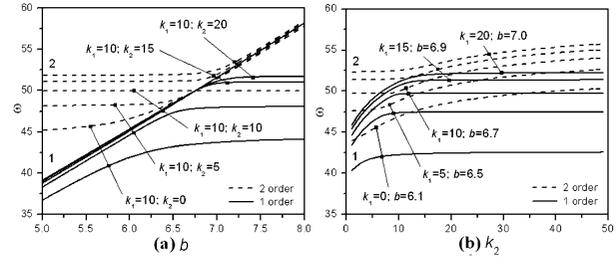


图3 最低两阶频率随(a)矢高和(b)弹簧刚度的变化示意图

Fig. 3 Variations of the first two frequencies with

(a) arch rise and (b) elastic stiffness

由图2可知 $k_1 = 10$ 而 k_2 取不同值时, 1:1 内共振的出现形式完全不同且对应参数存在差异, 为进一步研究转动弹簧刚度的影响, 图3(a)以最低两阶模态间的1:1内共振为研究对象给出了 k_1 和 k_2 取几组不同值时随变化的分布规律, 图中5组数据显示当 $k_1 \neq k_2$ 时两阶模态之间出现转向, $k_1 = k_2 = 10$ 时则出现交叉. 结合图2中的结果, 这说明当两端转动弹簧刚度相同结构完全对称时可能出现模态交叉, 而两端弹簧刚度不同结构不对称时则出现模态转向. 图3(b)则给出了 k_1 从0到20以公差5递增的5组数据中 ω 随 k_2 变化的示意图, 图中 b 取相应 k_1 和 $k_2 = 10$ 时最低两阶模态发生1:1内共振的值, 即 b 分别等于6.1, 6.5, 6.7, 6.9和7.0, 从图中可发现在 k_2 增至一定值时频率值趋于稳定, 两阶模态的频率值除 $k_1 = 10, b = 6.7$ 这组数据在 $k_2 = 10$ 附近接近外均有不同大小的差值, 这说明了内共振以模态转向形式为主.

图4则给出了 $k_1 = 10, k_2 = 20$ 时最低两阶频率在转向附近的正交模态分布示意图, 可发现模态既非正对称也非反对称而是由二者组合而成, 当 b 小于模态转向值7.0时1阶模态以对称成分为主, 2阶模态以反对称成分为主, 当 $b > 7.0$ 时则刚好相反.

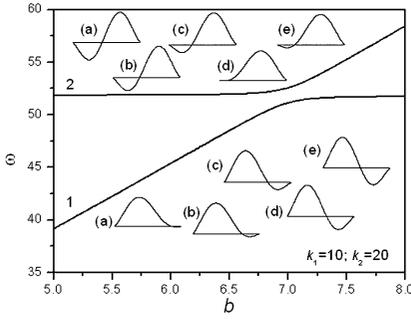


图4 最低两阶频率在转向位置附近的模态分布:

(a) = 6.8, (b) = 6.9, (c) = 7.0, (d) = 7.1, (e) = 7.2

Fig. 4 Variations of the first two frequencies along with the associated mode shapes with arch rise: (a) = 6.8, (b) = 6.9, (c) = 7.0, (d) = 7.1 and (e) = 7.2

2 内共振的摄动分析

为摄动分析方便将方程(5)写为如下形式

$$\begin{cases} \dot{u} - \nu = 0 \\ \dot{\nu} + Lu = G_2(u, u) + G_3(u, u, u) - \\ \varepsilon^2 c\dot{u} - \varepsilon^3 F \cos \Omega t \end{cases} \quad (10)$$

式中上标点表示对 t 的微分, G_2 和 G_3 分别为二次、三次非可换非线性微分算子, 其表达式为 $G_2(u, \nu) = u'' \langle \nu', \psi' \rangle + (1/2)\psi'' \langle u', \nu' \rangle$, $G_3(u, \nu, w) = (1/2) \langle \nu', w' \rangle$, 上标撇表示对 x 的微分. 采用多尺度法对其进行分解, 将 u 和 ν 的解直接一致展开为

$$\begin{cases} u(x, t) = \varepsilon u_1(x, T_0, T_1, T_2) + \\ \varepsilon^2 u_2(x, T_0, T_1, T_2) + \varepsilon^3 u_3(x, T_0, T_1, T_2) + \dots \\ \nu(x, t) = \varepsilon \nu_1(x, T_0, T_1, T_2) + \\ \varepsilon^2 \nu_2(x, T_0, T_1, T_2) + \varepsilon^3 \nu_3(x, T_0, T_1, T_2) + \dots \end{cases} \quad (11)$$

式中时间 $T_0 = t, T_1 = \varepsilon t, T_2 = \varepsilon^2 t$, 且有 $\partial/\partial t = D_0 + \varepsilon^1 D_1 + \varepsilon^2 D_2 + \dots, D_n = \partial/\partial T_n$. 将其代入(10)式展开并利用时间参数的独立性可得近似方程如下

$$\varepsilon: \begin{cases} D_0 u_1 - \nu_1 = 0 \\ D_0 \nu_1 + Lu_1 = 0 \end{cases} \quad (12)$$

$$\varepsilon^2: \begin{cases} D_0 u_2 - \nu_2 = -D_1 u_1 \\ D_0 \nu_2 + Lu_2 = -D_1 \nu_1 + G_2(u_1, u_1) \end{cases} \quad (13)$$

$$\varepsilon^3: \begin{cases} D_0 u_3 - \nu_3 = -D_2 u_1 - D_1 u_2 \\ D_0 \nu_3 + Lu_3 = -D_2 \nu_1 - D_1 \nu_2 + \\ G_2(u_1, u_2) + G_2(u_2, u_1) + \\ G_3(u_1, u_1, u_1) - c\nu_1 - F \cos \Omega t \end{cases} \quad (14)$$

上述方程组对应的边界条件均为(6)和(7), 对于 m 和 n 阶模态之间的相互作用, 内共振只与这两阶模态有关, 因此可以将一阶近似方程(12)的解表示为

$$\begin{cases} u_1 = A_m(T_1, T_2) e^{i\omega_m T_0} \phi_m(x) + \\ A_n(T_1, T_2) e^{i\omega_n T_0} \phi_n(x) + cc \\ \nu_1 = i\omega_m A_m(T_1, T_2) e^{i\omega_m T_0} \phi_m(x) + \\ i\omega_n A_n(T_1, T_2) e^{i\omega_n T_0} \phi_n(x) + cc \end{cases} \quad (15)$$

此处 A_k 表示 k 阶复模态的幅值, cc 表示前面项的共轭项, 将上式代入二阶近似方程(13)可得

$$D_0 u_2 - \nu_2 = -D_1 A_m e^{i\omega_m T_0} \phi_m - D_1 A_n e^{i\omega_n T_0} \phi_n + cc \quad (16)$$

$$\begin{aligned} D_0 \nu_2 + Lu_2 = & -i\omega_m D_1 A_m e^{i\omega_m T_0} \phi_m - i\omega_n D_1 A_n e^{i\omega_n T_0} \phi_n + \\ & [A_m^2 e^{2i\omega_m T_0} + A_m \bar{A}_m] G_2(\phi_m, \phi_m) + \\ & [A_m A_n e^{i(\omega_m + \omega_n) T_0} + A_n \bar{A}_m e^{i(\omega_n - \omega_m) T_0}] \times \\ & [G_2(\phi_m, \phi_n) + G_2(\phi_n, \phi_m)] + \\ & [\bar{A}_n e^{2i\omega_n T_0} + A_n \bar{A}_n] G_2(\phi_n, \phi_n) + cc \end{aligned} \quad (17)$$

外激励通过共振对系统输入能量, 假设 $\Omega = \omega_m + \varepsilon^2 \sigma_1, 1:1$ 内共振时 m 和 n 阶模态的接近程度 $\omega_n = \omega_m + \varepsilon^2 \sigma_2$, 调谐参数 σ_1 既可大于零也可小于零, 而 σ_2 则与内共振形式有关, 它在模态转向时间不改变符号. 已有研究^[14]表明 $1:1$ 内共振解与时间尺度 T_1 无关, 方程(16, 17)中 $D_1 A_m$ 和 $D_1 A_n$ 均为零, 共振项不在二阶近似方程中出现, 因此二阶近似解可表示为

$$\begin{aligned} u_2 = & A_m^2 e^{2i\omega_m T_0} \Psi_{mm}(x) + A_m \bar{A}_m \chi_{mm}(x) + \\ & A_n^2 e^{2i\omega_n T_0} \Psi_{nn}(x) + A_n \bar{A}_n \chi_{nn}(x) + \\ & A_n A_m e^{i(\omega_n + \omega_m) T_0} \Psi_{mn}(x) + \\ & A_n \bar{A}_m e^{i(\omega_n - \omega_m) T_0} \chi_{mn}(x) + cc \end{aligned} \quad (18)$$

$$\begin{aligned} \nu_2 = & A_m^2 e^{2i\omega_m T_0} \eta_{mm}(x) + A_m \bar{A}_m \zeta_{mm}(x) + \\ & A_n^2 e^{2i\omega_n T_0} \eta_{nn}(x) + A_n \bar{A}_n \zeta_{nn}(x) + \\ & A_n A_m e^{i(\omega_n + \omega_m) T_0} \eta_{mn}(x) + \\ & A_n \bar{A}_m e^{i(\omega_n - \omega_m) T_0} \zeta_{mn}(x) + cc \end{aligned} \quad (19)$$

其中 $\Psi_{kk}(\chi_{kk})$ 和 $\eta_{kk}(\zeta_{kk})$ 分别是二阶位移和速度形函数, 将上式代入式(16, 17)可得已解耦的位移形函数的边值微分方程

$$\begin{aligned} L\Psi_{mm} - 4\omega_m^2 \Psi_{mm} = & G_2(\phi_m, \phi_m); \\ L\Psi_{nn} - 4\omega_n^2 \Psi_{nn} = & G_2(\phi_n, \phi_n) \end{aligned} \quad (20)$$

$$\begin{aligned} L\Psi_{mn} - (\omega_m + \omega_n)^2 \Psi_{mn} = \\ G_2(\phi_m, \phi_n) + G_2(\phi_n, \phi_m) \end{aligned} \quad (21)$$

$$L\chi_{mm} = G_2(\phi_m, \phi_m); \quad L\chi_{nn} = G_2(\phi_n, \phi_n) \quad (22)$$

$$L\chi_{mn} - (\omega_n - \omega_m)^2 / \chi_{mn} = G_2(\phi_m, \phi_n) + G_2(\phi_n, \phi_m) \quad (23)$$

边界条件仍为(6)和(7),相应二阶速度场的形函数为

$$\eta_{mm} = 2i\omega_m \Psi_{mm}; \quad \eta_{nn} = 2i\omega_n \Psi_{nn};$$

$$\eta_{mn} = i(\omega_m + \omega_n) \Psi_{mn}; \quad (24)$$

$$\zeta_{mm} = \zeta_{nn} = 0; \quad \zeta_{mn} = i(\omega_n - \omega_m) \chi_{mn} \quad (25)$$

将二阶近似解(18),(19)和一阶近似解(15)代入三阶近似方程,并利用消除久期项条件的可以得到求解方程如下

$$2i\omega_m (D_2 A_m + \mu_m A_m) = K_1 A_n^2 \bar{A}_m e^{i\sigma_2 t} + K_2 A_m^2 \bar{A}_n e^{-i\sigma_2 t} + 2K_2 A_m \bar{A}_m A_n e^{i\sigma_2 t} + K_3 A_n^2 \bar{A}_m e^{2i\sigma_2 t} + K_{mm} A_m^2 \bar{A}_m + K_{mn} A_m A_n \bar{A}_n - \frac{1}{2} f_m e^{i\sigma_1 t} \quad (26)$$

$$2i\omega_n (D_2 A_n + \mu_n A_n) = K_1 A_n^2 \bar{A}_m e^{i\sigma_2 t} + 2K_1 A_m A_n \bar{A}_n e^{-i\sigma_2 t} + K_2 A_m^2 \bar{A}_m e^{-i\sigma_2 t} + K_3 A_m^2 \bar{A}_n e^{-2i\sigma_2 t} + K_{mn} A_m \bar{A}_m A_n + K_{nn} A_n^2 \bar{A}_n - \frac{1}{2} f_n e^{i(\sigma_1 - \sigma_2)t} \quad (27)$$

式中 K_{mm}, K_{nn}, K_{mn} 是与共振无关的系数, K_1, K_2, K_3 是与共振相关的作用系数,其具体表达式见附录(B1-B5)式, $f_k = \langle F, \phi_k \rangle, 2\mu_k = \langle c, \phi_k^2 \rangle$ ($k = m, n$), 将摄动解 A_k 写为极坐标形式

$$(A_m, A_n) = \frac{1}{2} (a_m, a_n) \exp \{ i[\beta_m + \sigma_1 t, \beta_n + (\sigma_1 - \sigma_2)t] \} \quad (28)$$

其中 a_j 和 β_j 均为实函数,将其代入可解性条件(26)式和(27)式,并将结果分成实部和虚部,整理之后可得极坐标形式的平均方程

$$\dot{a}_m = -\mu_m a_m - \frac{K_1}{8\omega_m} a_n^3 \sin\gamma_1 - \frac{K_2}{8\omega_m} a_m^2 a_n \sin\gamma_1 - \frac{K_3}{8\omega_m} a_m a_n^2 \sin 2\gamma_1 + \frac{f_m}{2\omega_m} \sin\beta_m \quad (29a)$$

$$a_m \dot{\beta}_m = -\sigma_1 a_m - \frac{K_{mm}}{8\omega_m} a_m^2 - \frac{K_{mn}}{8\omega_m} a_m a_n^2 - \frac{K_1}{8\omega_m} a_n^3 \cos\gamma_1 - \frac{3K_2}{8\omega_m} a_m^2 a_n \cos\gamma_1 - \frac{K_3}{8\omega_m} a_m a_n^2 \cos 2\gamma_1 + \frac{f_m}{2\omega_m} \cos\beta_m \quad (29b)$$

$$\dot{a}_n = -\mu_n a_n + \frac{K_1}{8\omega_n} a_n^2 a_m \sin\gamma_1 + \frac{K_2}{8\omega_n} a_m^3 \sin\gamma_1 + \frac{K_3}{8\omega_n} a_n a_m^2 \sin 2\gamma_1 + \frac{f_n}{2\omega_n} \sin\beta_n \quad (29c)$$

$$a_n \dot{\beta}_n = -(\sigma_1 - \sigma_2) a_n - \frac{K_{nn}}{8\omega_n} a_n^3 - \frac{K_{mn}}{8\omega_n} a_n a_m^2 - \frac{3K_1}{8\omega_n} a_n^2 a_m \cos\gamma_1 - \frac{K_2}{8\omega_n} a_m^3 \cos\gamma_1 - \frac{K_3}{8\omega_n} a_n a_m^2 \cos 2\gamma_1 + \frac{f_n}{2\omega_n} \cos\beta_n \quad (29d)$$

式中 $\gamma_1 = \beta_m - \beta_n$.

3 数值分析

在对转动弹簧弹性支撑浅拱的分岔进行数值研究时,以最低两阶模态($m=1, n=2$)发生模态转向1:1内共振附近的非线性响应为研究对象,系统参数假设为 $k_1=10, k_2=20, b=7.0, \mu_m=0.006, \mu_n=0.008, \omega_m=51.11, \omega_n=52.49$,平均方程中的各个系数如表1所示.

表1 平均方程系数表

Table 1 The coefficients of the averaging equation

| K_{mm} | K_{nn} | K_{mn} | K_1 | K_2 | K_3 |
|----------|----------|----------|--------|--------|---------|
| 1429.58 | 873.61 | 653.47 | -55.38 | 618.69 | -461.37 |

平均方程的稳态解或固定点可通过在式(29)中令 $\dot{a}_m = \dot{a}_n = \dot{\beta}_m = \dot{\beta}_n = 0$ 来获取,在确定稳态解的响应时一般先选取一个较大或较小的远离共振区的参数值,再利用 Newton-Raphson 法进行积分得到一组解,然后利用拟弧长的延拓法^[15]确定整条曲线.解的稳定性则由对应 4×4 Jacobian 矩阵的特征值予以判断,在下面稳态解中实线表示稳定解,虚线表示不稳定解.

3.1 激励幅值的影响

对于平均方程式(29)中的外激励,设 $f_1 = \langle F, \phi_1 \rangle, f_2 = 0$ 来分析激励幅值 F 发生变化时系统的响应,图5(a),(b)给出了 $\sigma_1=0, \sigma_2=0$ 和 $\sigma_1=0, \sigma_2=0.10$ 时 a_1 和 a_2 随 F 增大时的变化规律.在图5(a)中可以看到系统的稳态响应值随 F 的增大而单调增加,且稳态解一直为稳定解.对于 $\sigma_2=0.10$ 的情形,图5(b)所示激励响应曲线完全呈现另一番景象,从原点出发的稳定路径在 $F=0.77$ 和 $F=1.12$ 时分别遇到第1个和第2个 Hopf 分岔点,两个分岔点之间是不稳定解,随着 F 的增加稳态解单调增长至 $F=4.59$ 遇到第一个鞍结分岔点 $SN1$,接下来曲线以不稳定解折回至第3个 Hopf 分岔点,对应 $F=0.89$,然后稳态解曲线再经过两个鞍

结分岔点 $SN2 (F = 1.46)$ 和 $SN3 (F = 0.79)$ 以稳定 - 不稳定 - 稳定方式交替往返进入稳定状态。

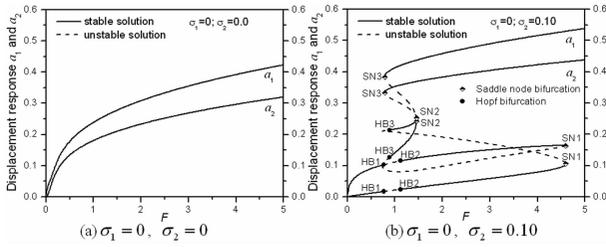


图5 激励幅值响应曲线 ($f_2 = 0$)

Fig. 5 Force - response curves for with $f_2 = 0$

3.2 激励频率的影响

图6给出了 $F = 3, f_2 = 0$ 和 $\sigma_2 = 0.05$ 时激励响应 a_1 和 a_2 随 σ_1 变化的幅频曲线. 由图可知随着的变化稳态响应的解存在有两条路径, 第一条路径在 σ_1 很小时是稳定解, 随 σ_1 的增长稳定性止于鞍结分岔点 $SN1$ (此时 $\sigma_1 = -0.20$), 此过程中 a_2 的幅值非常小, 所以结构的非线性响应可以忽略这一部分的影响, 经过 $SN1$ 后稳态解变得不稳定直至随 σ_1 减小达到另一个鞍结分岔点, 然后随着 σ_1 增加稳态解曲线经过两个 Hopf 分岔点 $HB1 (\sigma_1 = -0.30)$ 和 $HB2 (\sigma_1 = -0.21)$ 达到鞍结分岔点 $SN2 (\sigma_1 = -0.04)$, 两个 Hopf 分岔点之间的稳态解是不稳定的, 由 $SN2$ 出发的不稳定解曲线随 σ_1 的变化达到第三个 Hopf 分岔点 $HB3 (\sigma_1 = -0.06)$, 这条路径再由 $SN3$ 和另外一个鞍结分岔点最终进入远离共振区的恒稳状态, 此时位移响应以 a_1 为主, a_2 的影响可以忽略, 这条路径中两阶模态的幅频曲线均呈双支软弹簧性质, 这与平均方程中对幅频曲线起决定作用的系数 K_{mm} 和 K_{nn} 的符号相同有关. 第二条路径是一条闭合路径, 它被两个鞍结分岔点 $SN4 (\sigma_1 = -0.86)$ 和 $SN5 (\sigma_1 = -0.04)$ 分为一条稳定解和一条不稳定解两个部分.

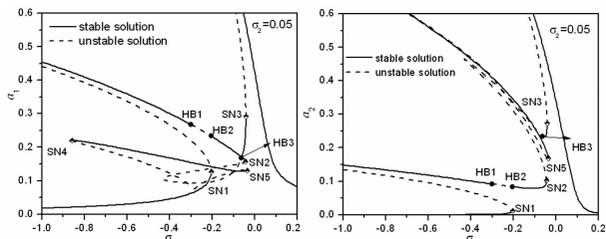


图6 频率响应曲线 ($F = 3; f_2 = 0; \sigma_2 = 0.05$)

Fig. 6 Frequency - response curves for,

$F = 3; f_2 = 0$ and $\sigma_2 = 0.05$

平均方程出现 Hopf 分岔之后, 稳态解将变为周期解, 相空间出现极限环, 本文利用 Shooting 法^[15]与数值积分求解两点边值问题得到系统的周期解, 并用 Floquet 理论^[15]来判断解的稳定性. 图6模态响应的幅频曲线中有3个 Hopf 分岔点, 以此为起点计算得到整条周期解曲线如图7(a)所示, 周期解分支中实心圆代表稳定解, 空心圆代表不稳定解. 从中可以看到以 $HB1$ 和 $HB2$ 出发的周期解分支中解是稳定的, 随着 σ_2 变化至 -0.26 时衍生出另外两条周期解分支, 其中一条稳定另外一条不稳定. 从 $HB3$ 出发的周期解分布十分复杂, 图7(b)所示的周期 T 说明系统除了周期解外还存在准周期解和混沌解.

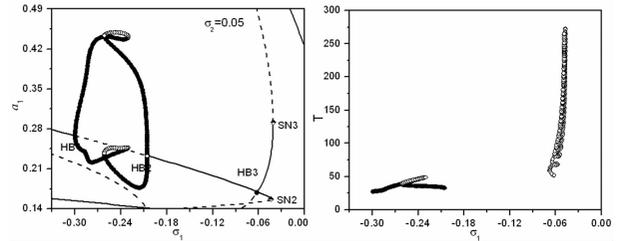


图7 内共振的周期解 ($F = 3; f_2 = 0; \sigma_2 = 0.05$)

Fig. 7 The period solutions of internal resonances with $F = 3, f_2 = 0$ and $\sigma_2 = 0.05$

3.3 调谐参数的影响

图8给出了 $\sigma_1 = -0.1, 0, 0.1$ 三种情况下 a_1 和 a_2 随着调谐参数 σ_2 变化的幅频曲线. 从中可知

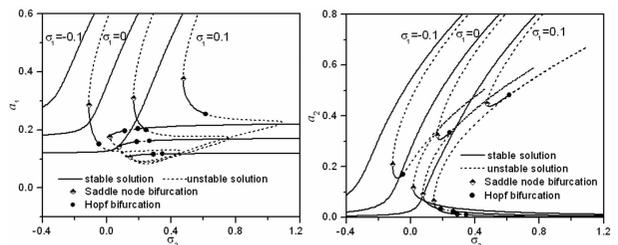


图8 σ_2 变化时的幅频曲线 ($F = 3; f_2 = 0$)

Fig. 8 Frequency - response curves for internal resonances with $F = 3$ and $f_2 = 0$

σ_1 取三种不同值时两阶模态的响应曲线在共振区的主要部分均呈硬弹簧性质; 另一方面在远离共振区系统的2阶模态响应值很小, 离共振区越远值越小, 非线性响应中可以忽略这一部分的影响. 三组稳态解在硬弹簧的下支不稳定解越过一个鞍结分岔点后均进入一段较短的稳定稳态解, 且稳定性都

止于一个 Hopf 分岔点,不稳定解接下来随 σ_2 的增大增至某一个值时再返回到一个鞍结分岔点,接下来随着 σ_2 增加则进入远离共振区的恒稳状态,期间还经过两个 Hopf 分岔点和这两个点之间的一段不稳定区域. σ_1 取不同值时三组解在整体上分布规律是一致的,只是表示其特征的具体值大小有差异.

4 结论

本文研究了浅拱在两端采用转动弹簧支撑的边界条件下,外激励引起系统出现内共振时的非线性动力学行为. 首先通过研究弹性支撑边界条件下自振频率及模态的分布规律,发现在一定条件下可发生模态交叉和转向的内共振. 以最低两阶模态之间的 1:1 内共振为研究对象,分析了模态转向时的动力学行为,分析过程中采用多尺度法对动力方程进行摄动求解,得到极坐标形式的平均方程. 通过外激励幅值、频率以及内部调谐参数对系统响应的研究研究了系统的稳态解和周期解,结果显示在转角弹性约束的浅拱中当主要参数处在某一范围之内时,外激励激发的模态相互作用将导致系统出现准周期运动和混沌运动.

参 考 文 献

- 1 项海帆,刘光栋. 拱结构的稳定与振动. 北京:人民交通出版社,1991 (Xiang H F, Liu G D. Stability and vibration of arch. Beijing: China Communications Press, 1991 (in Chinese))
- 2 易壮鹏,赵跃宇. 圆弧拱考虑一般缺陷的面内屈曲. 应用力学学报, 2009, 26(4): 721 ~ 724 (Yi Z P, Zhao Y Y. In-plane buckling of circular arch considering general imperfections. *Chinese Journal of Applied Mechanics*, 2009, 26(4): 721 ~ 724 (in Chinese))
- 3 Pi Y L, Bradford M A. Nonlinear in-plane elastic buckling of shallow circular arches under uniform radial and thermal loading. *International Journal of Mechanical Sciences*, 2010, 52(1): 75 ~ 88
- 4 程鹏,童根树. 圆弧拱平面内弯曲失稳一般理论. 工程力学, 2005, 22(1): 93 ~ 101 (Cheng P, Tong G S. A general theory for in-plane nonlinear analysis of circular arches. *Engineering Mechanics*, 2005, 22(1): 93 ~ 101 (in Chinese))
- 5 谢旭,李辉,黄剑源. 大跨度两铰钢拱桥面内稳定分析. 土木工程学报, 2004, 37(8): 43 ~ 49 (Xie X, Li H, Huang J Y. Study on in-plane stability of long-span two-hinged steel arch bridges. *China Civil Engineering Journal*, 2004, 37(8): 43 ~ 49 (in Chinese))
- 6 Chen J S, Lin J S. Dynamic snap-through of a shallow arch under a moving point load. *ASME, Journal of Vibration and Acoustics*, 2004, 126: 514 ~ 519
- 7 Chen J S, Li Y T. Effects of elastic foundation on the snap-through buckling of a shallow arch under a moving point load. *International Journal of Solids and Structures*, 2006, 43(14-15): 4220 ~ 4237
- 8 Tien W M, Namachchivaya N S, Bajaj A K. Non-linear dynamics of a shallow arch under periodic excitation-I. 1:1 internal resonance. *International Journal of Non-linear Mechanics*, 1994 29(3): 367 ~ 386
- 9 Lacarbonara W, Chin C M, Soper R R. Open-loop nonlinear vibration control of shallow arches via perturbation approach. *ASME, Journal of Applied Mechanics*, 2002, 69(3): 325 ~ 334
- 10 易壮鹏,康厚军,王连华. 基于 Kelvin 模型的粘弹性浅拱的动力稳定性. 动力学与控制学报, 2009, 7(3): 212 ~ 216 (Yi Z P, Kang H J, Wang L H. The dynamic behaviors of viscoelastic shallow arches based on Kelvin model. *Journal of Dynamics and Control*, 2009, 7(3): 212 ~ 216 (in Chinese))
- 11 钱长照,李寅磊,刘扬. 弹性支撑梁在移动荷载作用下的响应分析. 动力学与控制学报, 2011, 9(2): 162 ~ 166 (Qian C Z, Li Y L, Liu Y. Response of bridge with elastic bearing under moving load. *Journal of Dynamics and Control*, 2011, 9(2): 162 ~ 166 (in Chinese))
- 12 陈万祥,郭志昆. 粘弹性边界梁在低速冲击下的动力响应分析. 振动与冲击, 2008, 27(12): 69 ~ 72 (Chen W X, Guo Z K. Dynamic responses of beams with flexible supports subjected to low velocity impact. *Journal of Vibration and Shock*, 2008, 27(12): 69 ~ 72 (in Chinese))
- 13 Nayfeh A H, Pai P F. Linear and nonlinear structural mechanics. New York: Wiley-Interscience, 2004
- 14 Lacarbonara W, Rega G, Nayfeh A H. Resonant non-linear normal modes. Part I: analytical treatment for structural one-dimensional systems. *International Journal of Non-linear Mechanics*, 2003, 38: 851 ~ 871
- 15 Nayfeh A H, Balachandran B. Applied nonlinear dynamics. New York: Wiley-Interscience, 1994

RESEARCH ON THE NONLINEAR DYNAMIC BEHAVIORS OF ELASTIC SUPPORT SHALLOW ARCH*

Yi Zhuangpeng^{1†} Kang Houjun² Wang Lianhua²

(1. School of Civil Engineering and Architecture, Changsha University of Science and Technology. Changsha 410114, China)

(2. College of Civil Engineering, Hunan University. Changsha 410082, China)

Abstract The nonlinear dynamic behaviors of an elastic support hinged-hinged uniform shallow arch with two torsional springs located at two ends respectively under external excitation are investigated. Based on the control equation of elastic support shallow arch the multiple scale method was used for the perturbation analysis of internal resonances, and the averaging equation with its polar form was determined. The influence of the stiffness for elastic boundary, which has a one-to-one relationship to the corresponding coefficient in the averaging equation, can be reflected in the natural frequencies and mode shapes of arch structure via the characteristic equation. Then the 1:1 internal resonance between the lowest two modes was selected as studying object for numerical calculation. The analytical results show that there exist internal resonance forms for both cross and veer in the torsional elastic support shallow arch, further the two-mode interaction induced by external excitation may lead to quasi-periodic oscillation and chaotic motion when the systematical parameters are controlled in a certain range.

Key words shallow Arches, torsional elastic support, internal resonance, bifurcation, veer

附录

$$c_1 + c_3 = 0 \quad (A1)$$

$$\omega c_1 + k_1 \omega^{1/2} c_2 - \omega c_3 + k_1 \omega^{1/2} c_4 + k_2 \pi c_5 = 0 \quad (A2)$$

$$\cos \omega^{1/2} c_1 + \sin \omega^{1/2} c_2 + \cosh \omega^{1/2} c_3 + \sinh \omega^{1/2} c_4 = 0 \quad (A3)$$

$$\begin{aligned} & (\omega \cos \omega^{1/2} - k_2 \omega^{1/2} \sin \omega^{1/2}) c_1 + (\omega \sin \omega^{1/2} - \\ & k_s \omega^{1/2} \cos \omega^{1/2}) c_2 - (\omega^{1/2} \cosh \omega^{1/2} + \\ & k_2 \omega^{1/2} \sinh \omega^{1/2}) c_3 - (\omega^{1/2} \sinh \omega^{1/2} + \\ & k_2 \cosh \omega^{1/2}) c_4 + k_2 \pi c_5 = 0 \end{aligned} \quad (A4)$$

$$b^2 \pi^3 \omega (\Gamma_1 c_1 + \Gamma_2 c_2 + \Gamma_3 c_3 + \Gamma_4 c_4) + \Gamma_5 c_5 = 0 \quad (A5)$$

其中

$$\Gamma_1 = \frac{(1 + \cos \omega^{1/2})}{\pi^2 - \omega}, \Gamma_2 = \frac{\sin \omega^{1/2}}{\pi^2 - \omega}, \Gamma_3 = -\frac{(1 + \cosh \omega^{1/2})}{\pi^2 + \omega},$$

$$\Gamma_4 = -\frac{\sinh \omega^{1/2}}{\pi^2 + \omega}, \Gamma_5 = \pi^4 \left(1 + \frac{b^2}{2}\right) - \omega^2$$

$$\begin{aligned} K_{hh} = & \langle \phi_h G_2(\phi_h, \Psi_{hh}) \rangle + \langle \phi_h G_2(\Psi_{hh}, \phi_h) \rangle + \\ & 2 \langle \phi_h G_2(\phi_h, \chi_{hh}) \rangle + 2 \langle \phi_h G_2(\chi_{hh}, \phi_h) \rangle + \\ & 3 \langle \phi_h G_3(\phi_h, \phi_h, \phi_h) \rangle \text{ for } h = m, n \end{aligned} \quad (B1)$$

$$\begin{aligned} K_{mm} = & \langle \phi_m G_2(\phi_m, \Psi_{mm}) \rangle + \langle \phi_m G_2(\Psi_{mm}, \phi_m) \rangle + \\ & \langle \phi_m G_2(\phi_m, \chi_{mm}) \rangle + \langle \phi_m G_2(\chi_{mm}, \phi_m) \rangle + \\ & 2 \langle \phi_m G_2(\phi_m, \chi_{mn}) \rangle + 2 \langle \phi_m G_2(\chi_{mn}, \phi_m) \rangle + \\ & 2 \langle \phi_m G_3(\phi_m, \phi_m, \phi_m) \rangle + 2 \langle \phi_m G_3(\phi_m, \phi_m, \phi_n) \rangle + \\ & 2 \langle \phi_m G_3(\phi_m, \phi_n, \phi_n) \rangle \end{aligned} \quad (B2)$$

$$\begin{aligned} K_1 = & \langle \phi_n G_2(\phi_m, \Psi_{nn}) \rangle + \langle \phi_n G_2(\Psi_{nn}, \phi_m) \rangle + \\ & \langle \phi_n G_2(\phi_n, \chi_{nn}) \rangle + \langle \phi_n G_2(\chi_{nn}, \phi_n) \rangle + \\ & \langle \phi_n G_3(\phi_n, \phi_n, \phi_m) \rangle + \langle \phi_n G_3(\phi_n, \phi_m, \phi_n) \rangle + \\ & \langle \phi_n G_3(\phi_m, \phi_n, \phi_n) \rangle \end{aligned} \quad (B3)$$

$$\begin{aligned} K_2 = & \langle \phi_n G_2(\phi_m, \Psi_{mm}) \rangle + \langle \phi_n G_2(\Psi_{mm}, \phi_m) \rangle + \\ & 2 \langle \phi_n G_2(\phi_m, \chi_{mm}) \rangle + 2 \langle \phi_n G_2(\chi_{mm}, \phi_m) \rangle + \\ & 3 \langle \phi_n G_3(\phi_m, \phi_m, \phi_m) \rangle \end{aligned} \quad (B4)$$

$$\begin{aligned} 2K_3 = & \langle \phi_n G_2(\phi_n, \Psi_{mm}) \rangle + \langle \phi_n G_2(\Psi_{mm}, \phi_n) \rangle + \\ & \langle \phi_n G_2(\phi_m, \chi_{mm}) \rangle + \langle \phi_n G_2(\chi_{mm}, \phi_m) \rangle + \\ & \langle \phi_n G_3(\phi_m, \phi_m, \phi_n) \rangle + \langle \phi_n G_3(\phi_m, \phi_n, \phi_m) \rangle + \\ & \langle \phi_n G_3(\phi_n, \phi_m, \phi_m) \rangle \end{aligned} \quad (B5)$$

Received 12 October 2012, revised 27 November 2012.

* The project supported by the National Science Foundation of China (11002030, 10972073, 11102063, 11032004), the program for New Excellent Talents in University (NCET-09-0335)

† Corresponding author E-mail: yizhuangpeng@163.com